Global climate stabilisation by chemical weathering during the Hirnantian glaciation

Philip Pogge von Strandmann[1*], Andre Desrochers[2], Melissa J. Murphy[3], Alexander J. Finlay[4,5], David Selby[6], Timothy M. Lenton[7]

[1]London Geochemistry and Isotope Centre, Institute of Earth and Planetary Sciences, University College London and Birkbeck, University of London, Gower Street, London, WC1E 6BT, UK.

[2]Department of Earth and Environmental Sciences, University of Ottawa, ON K1N 6N5, Canada.

[3]Department of Earth Sciences, University of Oxford, Oxford, OX1 3AN, UK.

[4]Chemostrat Ltd, Welshpool, SY21 8SL, UK.

[5]School of Earth and Environmental Sciences, University of Portsmouth, PO1 2UP

[6]Department of Earth Sciences, University of Durham, Durham, DH1 3LE, UK.

[7]College of Life and Environmental Sciences, University of Exeter, Exeter, EX4 4QE, UK.

[*]Corresponding email: p.strandmann@ucl.ac.uk

Chemical weathering of silicate rocks is a primary drawdown mechanism of atmospheric carbon dioxide. The processes that affect weathering are therefore central in controlling global climate. A temperature-controlled "weathering thermostat" has long been proposed in stabilising long-term climate, but without definitive evidence from the geologic record. Here we

use lithium isotopes (δ^7Li) to assess the impact of silicate weathering across a significant climate-cooling period, the end-Ordovician Hirnantian glaciation (~445 Ma). We find a positive δ^7Li excursion, suggestive of a silicate weathering decline. Using a coupled lithium-carbon model, we show that initiation of the glaciation was likely caused by declining CO_2 degassing, which triggered abrupt global cooling, and much lower weathering rates. This lower CO_2 drawdown during the glaciation allowed climatic recovery and deglaciation. Combined, the data and model provide support from the geological record for the operation of the weathering thermostat.

The recovery and stabilisation of Earth's climate system from perturbations is central to the continued survival of life. Chemical weathering of continental silicate rocks driving marine carbonate precipitation is the Earth's primary long-term mechanism for removal of atmospheric CO_2 (BERNER, 2003). A temperature feedback control on weathering rates (i.e. greater temperatures cause higher weathering rates, removing more CO_2) would result in a climate-stabilising mechanism. This "weathering thermostat" has long been postulated and assumed in models (COLBOURN *et al.*, 2015). However, direct evidence for weathering rate changes in response to climate perturbations has been harder to pin down in the geological record.

The Late Ordovician Hirnantian (~445 Ma) records the second largest mass extinction in Earth history. This was likely caused by rapidly decreasing temperatures, culminating in an ice-sheet over Gondwana (ELRICK *et al.*, 2013). As such, similarities exist between the Hirnantian and the Late Cenozoic

glaciations (GHIENNE *et al.*, 2014). The behaviour of atmospheric CO_2 is of particular interest, because of the potential role of declining CO_2 in initiating the glaciation and of increasing CO_2 in terminating it (VANDENBROUCKE *et al.*, 2010). Either or both could have involved changes in silicate weathering rates (BERNER, 2003). The combination of changes in weathering rates and pCO_2 also resulted in a global positive $\delta^{13}C$ excursion (HICE) (LENTON *et al.*, 2012; GHIENNE *et al.*, 2014). Osmium isotopes have suggested a decline in weathering during the glacial maximum (FINLAY *et al.*, 2010). However, Os mainly traces weathering provenance, rather than weathering rates or processes. Lithium isotopes are the only tracer available whose behaviour is solely controlled by silicate weathering processes, and therefore give a unique insight into CO_2 drawdown and climate-stabilisation.

Lithium isotopes (δ^7Li) are not fractionated by biological processes (POGGE VON STRANDMANN *et al.*, 2016), and are not affected by carbonate weathering (DELLINGER *et al.*, 2015). The δ^7Li of primary silicate rocks defines a narrow range (continental crust ~0.6 ± 0.6‰, basalt ~3–5‰ (SAUZEAT *et al.*, 2015)) compared to the high variability in modern rivers (2–44‰ (HUH *et al.*, 1998; DELLINGER *et al.*, 2015; POGGE VON STRANDMANN AND HENDERSON, 2015)). Riverine values reflect weathering processes, particularly the extent of preferential uptake of ^6Li into secondary minerals (DELLINGER *et al.*, 2015), and therefore reflect "weathering congruency", defined as the ratio of primary rock dissolution (driving rivers to low, rock-like, δ^7Li = congruent dissolution of rock), to secondary mineral formation (driving rivers to high δ^7Li)(MISRA AND FROELICH, 2012; POGGE VON STRANDMANN AND HENDERSON, 2015). In modern oceans, rivers (~50% of the ocean input, with a mean δ^7Li ~23‰ (HUH *et al.*, 1998)) are

combined with mid-ocean ridge hydrothermal solutions (~50%, with a mean δ^7Li ~7‰ (CHAN *et al.*, 1993)). The oceanic sinks are incorporation into low-temperature clays in altered oceanic basalt (AOC) and marine authigenic clays (MAAC), which cumulatively impose isotopic fractionation of ~15‰, driving modern seawater to 31‰. Marine carbonates represent a negligible sink for Li, and their isotopic fractionation factor remains approximately constant at ~3–5‰, independent of temperature, salinity, or whether the calcite is inorganic or skeletal (MARRIOTT *et al.*, 2004; POGGE VON STRANDMANN *et al.*, 2013).

Here we present δ^7Li from bulk carbonates and brachiopods from Anticosti Island, Canada (ACHAB *et al.*, 2013) (Pointe Laframboise and Ellis Bay West), and from an equivalent shale section at Dob's Linn, UK (FINLAY *et al.*, 2010; MELCHIN *et al.*, 2013) (see Supplement for methods and data). The δ^7Li values from all sections exhibit a positive excursion of ≤10‰ before the HICE (Fig. 1). We rule out effects on carbonate δ^7Li by silicate leaching, due to our processing technique (see Supplement). We also rule out diagenesis, because trends and absolute values of δ^7Li, δ^{13}C and δ^{18}O (MELCHIN *et al.*, 2013) are reproduced in different sections, both bulk carbonates and brachiopods (Fig. 1). Overall, therefore, this suggests that the Li isotopic excursion represents a primary seawater signal.

While carbonates tend to be the usual seawater archive (e.g. (MISRA AND FROELICH, 2012; POGGE VON STRANDMANN *et al.*, 2013), silicates have also been investigated (DELLINGER *et al.*, 2017), and sediments older than Ordovician are considered to represent pre-depositional (unaltered by diagenesis) weathering signals (LI *et al.*, 2016). Hence, detrital clays (which dominate at Dob's Linn) should reflect changing local continental weathering conditions (see Supplement

and Fig. S4). Tracers such as Si/Al, Li/Al or $^{187}Os/^{188}Os$ rule out control by changing provenance or clay mineralogy. Dob's Linn exhibits an isotope excursion of similar magnitude, but ~14‰ lower than the carbonates. While biostratigraphy suggests that the $\delta^{13}C_{carb}$ and $\delta^{13}C_{org}$ of Anticosti and Dob's Linn are slightly offset (MELCHIN *et al.*, 2013)(Fig. 1), in all sections the relative timings of the $\delta^{7}Li$ and HICE are similar. Chemostratigraphy therefore suggests the Li isotope excursions occur contemporaneously (see Supplement), consistent with lithium's long modern ocean residence time (~1 Myr). A simple temperature dependence of the clay fractionation factor during weathering would only cause <1.6‰ variation (LI AND WEST, 2014), and is therefore not the cause of the observed variability. Although shales, in particular clay fractionation factors, are under-constrained for a quantitative interpretation in isolation, their comparison to and temporal similarities with carbonates suggests a link. Thus, global seawater compositions (represented by carbonates) appear to be responding to the same driving force as this local archive of continental weathering (represented by shales).

The pre- and post-excursion $\delta^{7}Li_{seawater}$ values of ~15‰ are difficult to achieve in a modern ocean. It is likely that the AOC and MAAC sinks were broadly similar to today (HAZEN *et al.*, 2013), imparting an isotopic fractionation factor of ~15‰, which may be temperature-dependent, as discussed below. We do not consider a "sink-shift" between proportions of MAAC vs. AOC, as proposed for the Cenozoic (LI AND WEST, 2014), because the Hirnantian duration is likely too short (1–2 Myr) for a transient change. Therefore, Li inputs must have had an isotope ratio close to 0‰. Assuming a modern-like hydrothermal input, this requires that rivers had $\delta^{7}Li$ values essentially unfractionated from the

126 continental crust (modern value ~0‰ (SAUZEAT *et al.*, 2015)). This possibility is
127 supported by δ^7Li values of ~2‰ for the Amazon river (DELLINGER *et al.*, 2015),
128 and similarly low values during the peak of the Cenomanian-Turonian
129 hyperthermal (POGGE VON STRANDMANN *et al.*, 2013). However, data here imply
130 that Ordovician oceans were isotopically light at steady state. Given that the first
131 non-vascular land plants were only just evolving and colonising the continents in
132 the mid-late Ordovician (with associated organic acid production), it is probable
133 that clay types were different and less abundant (HAZEN *et al.*, 2013). For
134 example, illites, which cause little Li isotope fractionation (MILLOT AND GIRARD,
135 2007), are thought to dominate prior to terrestrialisation by plants (HAZEN *et al.*,
136 2013). If this is a feature of early Earth weathering, then the continental crust's
137 δ^7Li would have been mantle-like (~3‰), rather than driven isotopically light by
138 weathering.

139 Assuming, therefore, that silicate weathering was highly congruent, we
140 have created a dynamic non-steady-state coupled Li and C cycle model (see
141 Supplement). In brief, the model uses Li formulations from previous work (POGGE
142 VON STRANDMANN *et al.*, 2013; LECHLER *et al.*, 2015), with an added temperature
143 dependence on the Li sink with a sensitivity of -0.15‰/K (LI AND WEST, 2014),
144 and links the weathering flux to that calculated by the carbon cycle model (based
145 on GEOCARB III). Existing climate models suggest that pCO_2 needed to halve to
146 ~8PAL (present atmospheric level) to trigger the Hirnantian glaciation (POHL *et*
147 *al.*, 2016). This could be initiated by a decline in degassing (MCKENZIE *et al.*,
148 2016), an increase in plant cover (LENTON *et al.*, 2012) or uplift (KUMP *et al.*,
149 1999), or a combination of these. A rather extreme decline in degassing from the
150 initial Ordovician value of 1.55× to 0.75× modern causes CO_2 to drop to ~6.5PAL.

Both the hydrothermal and riverine Li fluxes scale proportionally to degassing, resulting in no steady-state change, but a transient adjustment of the oceanic Li reservoir causes a positive δ^7Li excursion of ~3.5‰ (i.e. correct direction, but smaller excursion). In contrast, increasing plant-induced weathering (and associated clay mineral formation) causes a permanent, rather than transient δ^7Li increase (see Supplement), which is not observed in our data. However, it is possible that the two processes operated in conjunction. A 65% increase in uplift would create the same effect, but would be unprecedented in the Phanerozoic. Theoretically, the excursion could also be caused by an increase in riverine δ^7Li by ~15‰ with no change in flux. However this is unlikely, because it implies greater uptake into clay minerals, which would cause a decrease in river flux. This scenario also has no carbon cycle forcing, and hence we prefer a coupled flux and isotope ratio change, initiated by a degassing change.

A recent insight is that a glacial "tipping point" existed in the Late Ordovician, where, once global temperature dropped to a critical threshold, northern high latitude sea-ice expanded abruptly, causing a further decrease in global temperatures and rapid expansion of an ice sheet on the Southern polar land surfaces (POHL *et al.*, 2016). These ice-albedo and heat transport feedbacks operate far faster than the long-term carbon cycle. Hence to represent this we implement an abrupt cooling when CO_2 reaches ~8PAL, generating reduced silicate weathering rates. To prevent an immediate abrupt warming, we assume some bi-stability of temperature and ice cover such that CO_2 has to rise to >8PAL before deglaciation occurs. The cooling-induced reduction in global weathering flux (by ~4×), causes an accelerated rise in δ^7Li from 17–19‰ (depending on continental crust composition) to >25‰ (Fig. 2), which is reversed when the

build-up of CO_2 triggers abrupt warming and deglaciation. Hence peak δ^7Li is predicted to be at the end of the glacial interval, consistent with sea-level reconstructions (Fig. 2). The size of the excursion could be increased by coupling the weathering decline with higher riverine δ^7Li, as suggested by the shale record (Fig. 2). This could be caused by an increase in the continental residence time of water allowing more clay formation, or a temperature-dependent shift in clay mineralogy. Such a change in congruency could also assist a vegetation-accelerated scenario, where terrestrialisation enhanced weathering, but enhanced glacial grinding forced a return to more congruent weathering. Such vegetative forcing would also cause a transient δ^7Li excursion (Fig. S9), albeit one of longer duration, hence we consider this less likely. Critically, the model can explain an increase in δ^7Li as cooling starts, but before the full glaciation was initiated, and the highest oceanic δ^7Li occurring at the end of the glaciation as observed in the record. $^{187}Os/^{188}Os$ values (FINLAY *et al.*, 2010) agree with this scenario, suggesting inhibition of weathering by cooling (which would also increase CO_2 (KUMP *et al.*, 1999)) and hence a change in provenance focus, coincident with the δ^7Li peak. Our model also predicts $^{87}Sr/^{86}Sr$ variation within the observed scatter (SHIELDS *et al.*, 2003), lending further credence to our interpretation (see Supplement).

The data and model are therefore consistent with the Hirnantian glaciation being initiated by declining CO_2 degassing, leading to a transient decline in silicate weathering, in turn causing an atmospheric CO_2 increase that ultimately terminated the glaciation. The Hirnantian has been compared to Cenozoic glaciations (GHIENNE *et al.*, 2014), where both periods are now characterised by increasing δ^7Li values (MISRA AND FROELICH, 2012). The positive

201 δ^7Li excursion during the Hirnantian cooling event also compares well to
202 negative δ^7Li excursions during warming events (POGGE VON STRANDMANN *et al.*,
203 2013; LECHLER *et al.*, 2015). Overall, therefore, this study shows that if a tectonic-
204 driven climate control (degassing) can push the climate system out of balance, a
205 temperature-dependent feedback via silicate weathering will eventually stabilise
206 the climate. Such a weathering thermostat has frequently been postulated as a
207 climate regulating process, but has proven remarkably difficult to
208 unambiguously demonstrate in the geological record.
209
210 Acknowledgements
211 This study and PPvS were funded by NERC advanced research fellowship
212 NE/I020571/2 and ERC Consolidator grant 682760 - CONTROLPASTCO2. AD
213 thanks the support of the Natural Science and Engineering Council of Canada
214 (Discovery Grant). TML was supported by NERC (NE/N018508/1). DS
215 acknowledges the Total Endowment Fund. Michael Melchin is thanked for
216 reading an earlier version of the manuscript. This manuscript was greatly
217 improved by reviews from Lee Kump, Jerome Gaillardet and an anonymous
218 reviewer.
219
220 Author contributions
221 PPvS wrote the research proposal, carried out the analyses and wrote the
222 manuscript. TML and PPvS conducted the modelling. AD, AJF and DS provided
223 samples, geochemical context and edited the manuscript. MJM assisted in
224 analyses and edited the manuscript.
225

Achab, A., Asselin, E., Desrochers, A., Riva, J.F. (2013) The end-Ordovician chitinozoan zones of Anticosti Island, Quebec: Definition and stratigraphic position. *Review of Palaeobotany and Palynology* 198, 92-109.

Berner, R.A. (2003) The long-term carbon cycle, fossil fuels and atmospheric composition. *Nature* 426, 323-326.

Chan, L.H., Edmond, J.M., Thompson, G. (1993) A lithium isotope study of hot springs and metabasalts from mid-ocean ridge hydrothermal systems. *Journal of Geophysical Research* 98, 9653-9659.

Colbourn, G., Ridgwell, A., Lenton, T.M. (2015) The time scale of the silicate weathering negative feedback on atmospheric CO2. *Global Biogeochemical Cycles* 29, 583–596.

Dellinger, M., Bouchez, J., Gaillardet, J., Faure, L., Moureau, J. (2017) Tracing weathering regimes using the lithium isotope composition of detrital sediments. *Geology* in press.

Dellinger, M., Gaillardet, J., Bouchez, J., Calmels, D., Louvat, P., Dosseto, A., Gorge, C., Alanoca, L., Maurice, L. (2015) Riverine Li isotope fractionation in the Amazon River basin controlled by the weathering regimes. *Geochimica Et Cosmochimica Acta* 164, 71–93.

Elrick, M., Reardon, D., Labor, W., Martin, J., Desrochers, A., Pope, M. (2013) Orbital-scale climate change and glacioeustasy during the early Late Ordovician (pre-Hirnantian) determined from delta O-18 values in marine apatite. *Geology* 41, 775-778.

Finlay, A.J., Selby, D., Grocke, D.R. (2010) Tracking the Hirnantian glaciation using Os isotopes. *Earth and Planetary Science Letters* 293, 339–348.

Ghienne, J.-F., Desrochers, A., Vandenbroucke, T.R.A., Achab, A., Asselin, E., Dabard, M.-P., Farley, C., Loi, A., Paris, F., Wickson, S., Veizer, J. (2014) A Cenozoic-style scenario for the end-Ordovician glaciation. *Nature Communications* 5.

Hazen, R.M., Sverjensky, D.A., Azzolini, D., Bish, D.L., Elmore, S.C., Hinnov, L., Milliken, R.E. (2013) Clay mineral evolution. *American Mineralogist* 98, 2007–2029.

Huh, Y., Chan, L.H., Zhang, L., Edmond, J.M. (1998) Lithium and its isotopes in major world rivers: Implications for weathering and the oceanic budget. *Geochimica Et Cosmochimica Acta* 62, 2039–2051.

Kump, L.R., Arthur, M.A., Patzkowsky, M.E., Gibbs, M.T., Pinkus, D.S., Sheehan, P.M. (1999) A weathering hypothesis for glaciation at high atmospheric pCO2 during the Late Ordovician *Palaeogeography, Palaeoclimatology, Palaeoecology* 152, 173-187.

Lechler, M., Pogge von Strandmann, P.A.E., Jenkyns, H.C., Prosser, G., Parente, M. (2015) Lithium-isotope evidence for enhanced silicate weathering during OAE 1a (Early Aptian Selli event). *Earth and Planetary Science Letters* 432, 210–222.

Lenton, T.M., Crouch, M., Johson, M., Pires, N., Dolan, L. (2012) First plants cooled the Ordovician. *Nature Geoscience* 5, 86–89.

Li, G., West, A.J. (2014) Evolution of Cenozoic seawater lithium isotopes: Coupling of global denudation regime and shifting seawater sinks. *Earth and Planetary Science Letters* 401, 284–293.

274 Li, S., Gaschnig, R.M., Rudnick, R.L. (2016) Insights into chemical weathering of
275 the upper continental crust from the geochemistry of ancient glacial
276 diamictites. *Geochimica Et Cosmochimica Acta* 176, 96–117.
277 Marriott, C.S., Henderson, G.M., Crompton, R., Staubwasser, M., Shaw, S. (2004)
278 Effect of mineralogy, salinity, and temperature on Li/Ca and Li isotope
279 composition of calcium carbonate. *Chemical Geology* 212, 5–15.
280 McKenzie, N.R., Horton, B.K., Loomis, S.E., Stockli, D.F., Planavsky, N.J., Lee, C.-T.A.
281 (2016) Continental arc volcanism as the principal driver of icehouse-
282 greenhouse variability. *Science* 352, 444–447.
283 Melchin, M.J., Mitchell, C.E., Holmden, C., Storch, P. (2013) Environmental
284 changes in the Late Ordovician-early Silurian: Review and new insights
285 from black shales and nitrogen isotopes. *Geological Society of America*
286 *Bulletin* 125, 1635-1670.
287 Millot, R., Girard, J.P. (2007) Lithium Isotope Fractionation during adsorption
288 onto mineral surfaces. *International meeting, Clays in natural & engineered*
289 *barriers for radioactive waste confinement* (Lille, Frace),
290 Misra, S., Froelich, P.N. (2012) Lithium Isotope History of Cenozoic Seawater:
291 Changes in Silicate Weathering and Reverse Weathering. *Science* 335,
292 818–823.
293 Pogge von Strandmann, P.A.E., Burton, K.W., Opfergelt, S., Eiriksdottir, E.S.,
294 Murphy, M.J., Einarsson, A., Gislason, S.R. (2016) The effect of
295 hydrothermal spring weathering processes and primary productivity on
296 lithium isotopes: Lake Myvatn, Iceland. *Chemical Geology* in press.
297 Pogge von Strandmann, P.A.E., Henderson, G.M. (2015) The Li isotope response
298 to mountain uplift. *Geology* 43, 67–70.
299 Pogge von Strandmann, P.A.E., Jenkyns, H.C., Woodfine, R.G. (2013) Lithium
300 isotope evidence for enhanced weathering during Oceanic Anoxic Event 2.
301 *Nature Geoscience* 6, 668–672.
302 Pohl, A., Donnadieu, Y., Le Hir, G., Ladant, J.-B., Dumas, C., Alvarez-Solas, J.,
303 Vandenbroucke, T.R.A. (2016) Glacial onset predated Late Ordovician
304 climate cooling. *Paleoceanography* 31, 800–821.
305 Sauzeat, L., Rudnick, R.L., Chauvel, C., Garcon, M., Tang, M. (2015) New
306 perspectives on the Li isotopic composition of the upper continental crust
307 and its weathering signature. *Earth and Planetary Science Letters* 428,
308 181–192.
309 Shields, G.A., Carden, G.A.F., Veizer, J., Meidla, T., Rong, J.-Y., Li, R.-Y. (2003) Sr, C,
310 and O isotope geochemistry of Ordovician brachiopods: A major isotopic
311 event around the Middle-Late Ordovician transition *Geochimica Et*
312 *Cosmochimica Acta* 67, 2005-2025.
313 Vandenbroucke, T.R.A., Armstrong, H.A., Williams, M., Paris, F., Zalasiewicz, J.A.,
314 Sabbe, K., Nolvak, J., Challandsa, T.J., Verniers, J., Servais, T. (2010) Polar
315 front shift and atmospheric CO2 during the glacial maximum of the Early
316 Paleozoic Icehouse. *Proceedings of the National Academy of Sciences of the*
317 *United States of America* 107, 14983-14986.
318

319

320

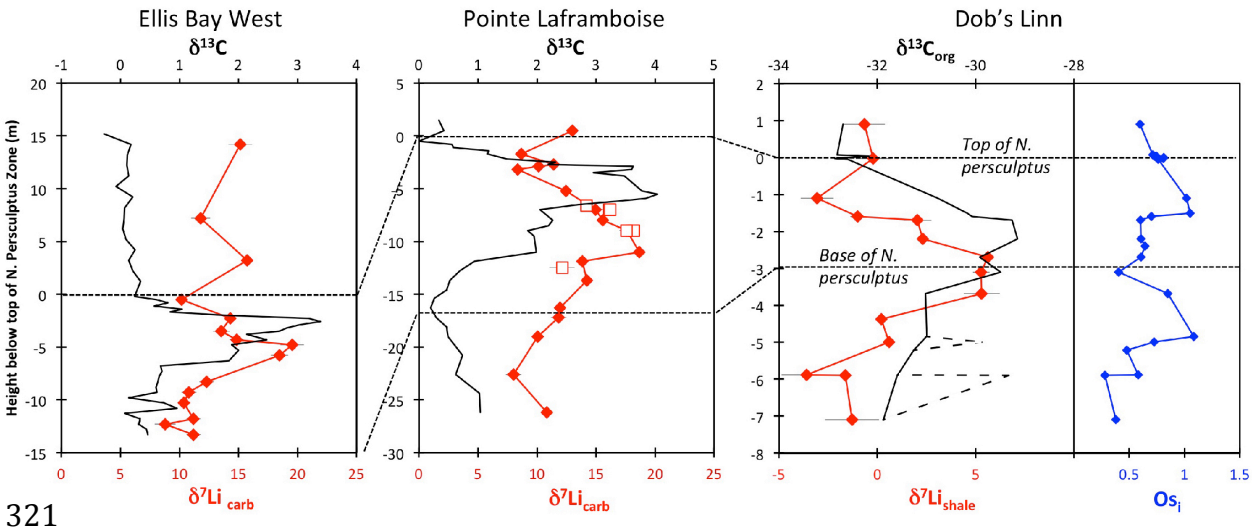

321

322 Figure 1. Carbonate (Pointe Laframboise and Ellis Bay West) and shale (Dob's
323 Linn) Li isotope ratios. Open squares are separately analysed brachiopods.
324 Carbon and osmium (initial $^{187}Os/^{188}Os$) isotope data are from the same samples
325 (FINLAY *et al.*, 2010). Biostratigraphic correlation is based on the N. persculptus
326 zone (MELCHIN *et al.*, 2013).

327

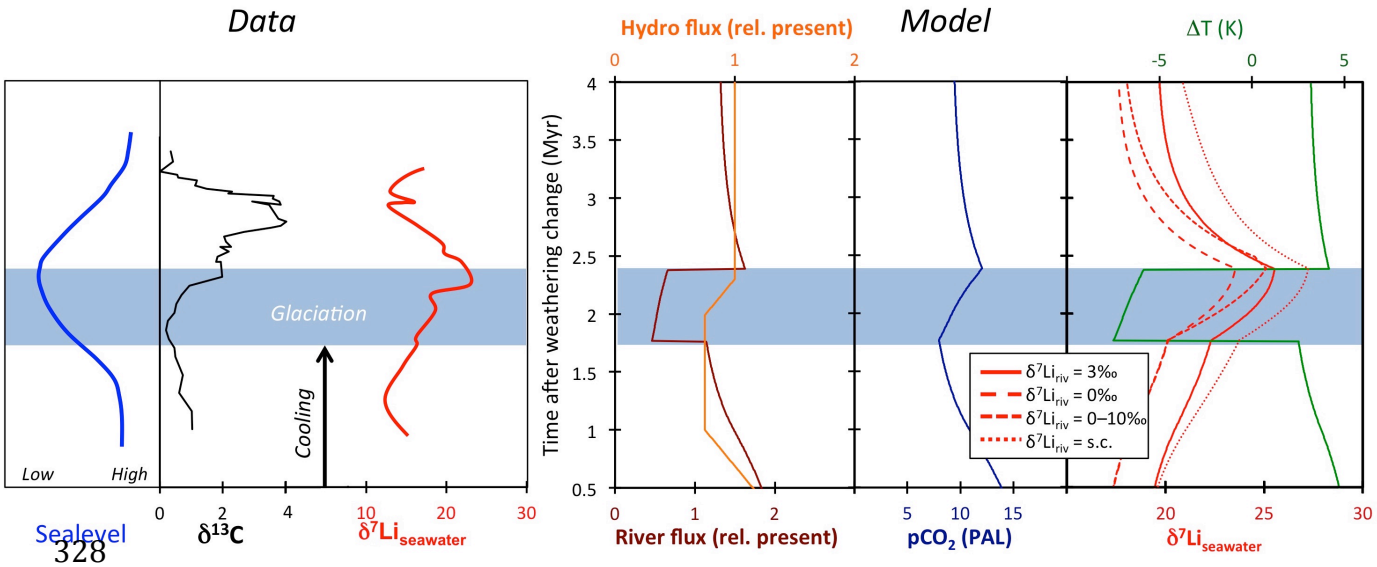

328

329 Figure 2. Comparison of data and model results. Sea level timing is from
330 stratigraphic data (GHIENNE *et al.*, 2014). Seawater Li isotope data were
331 generated from carbonate data by adding a 4‰ fractionation factor (MARRIOTT *et*

332 *al.*, 2004). The model shows the changes in riverine and hydrothermal Li fluxes,
333 the pCO_2 levels and temperature anomalies caused by these changes, and the
334 resulting oceanic δ^7Li curve. The red model lines are for scenarios where riverine
335 δ^7Li = 3‰, 0‰, a change from 0 to 10‰ during the glaciation and "shale-
336 constrained" (s.c.), using Dob's Linn δ^7Li data to constrain river values (see text
337 and supplement for detail).